Available online at www.sciencedirect.com
SCIENCE DIRECT®
Bioorganic & Medicinal Chemistry 13 (2005) 4425–4433
Bioorganic & Medicinal Chemistry

Phthalazine PDE IV inhibitors: Conformational study of some 6-methoxy-1,4-disubstituted derivatives

Thomas Haack,[a,*] Raimondo Fattori,[a] Mauro Napoletano,[a] Franco Pellacini,[a] Giovanni Fronza,[b] Giuseppina Raffaini[c] and Fabio Ganazzoli[c]

[a]*Inpharzam Ricerche, Zambon Group, Via ai Söi, 6807 Taverne, Switzerland*
[b]*CNR, Istituto di Chimica del Riconoscimento Molecolare, Dipartimento di Chimica, Materiali e Ingegneria Chimica 'G. Natta', Via Mancinelli 7, 20131 Milano, Italy*
[c]*Politecnico di Milano, Dipartimento di Chimica, Materiali e Ingegneria Chimica 'G. Natta', Via Mancinelli 7, 20131 Milano, Italy*

Received 26 January 2005; accepted 19 April 2005
Available online 31 May 2005

Abstract—This report describes the detailed conformational analysis and synthesis of a series of phthalazine phosphodiesterase-type (IV) (PDE IV) inhibitors bearing either mono- or dichloro 4-methylenepyridine at the 'down' position of the phthalazine nucleus or different heterocycles at the 'top' position 4 of the phthalazine moiety. Both the mono- and dichloro 4-methylenepyridine units linked at carbon C_1 of the phthalazine nucleus show identical conformational behaviour with the substituent preferentially oriented towards the external part of the molecule and the pyridine plane almost orthogonal to that of phthalazine ring. The heterocyclic five-membered rings linked at carbon C_4 of phthalazine show quite different conformational behaviour. The 1,3-thiazole ring exists in a well-defined conformation almost coplanar with respect to the phthalazine nucleus while the 1,2,4-triazole and the 1,3-diazole heterocycles show a great conformational freedom with large torsion angles. Compound **3** bearing the thiazole ring at C_4 displays the major biological activity, thus suggesting that a planar and rather rigid conformation of the pentacycle should favour the PDE IV inhibition capacity of this class of compounds.

1. Introduction

The phosphodiesterases (PDEs) are involved in intracellular degradation of cyclic adenosine monophosphate (cAMP) and cyclic guanosine monophosphate (cGMP) to form their corresponding 5′-monophosphates. Phosphodiesterase type IV (PDE IV) is a cAMP-specific phosphodiesterase highly expressed in inflammatory cells and in the airway smooth muscle.[1] The observation that an elevation of cAMP in these cells can suppress inflammatory effects and can induce muscle relaxation has stimulated great interest in developing selective PDE IV inhibitors as therapeutic agents for asthma or chronic obstructive pulmonary disease (COPD) and

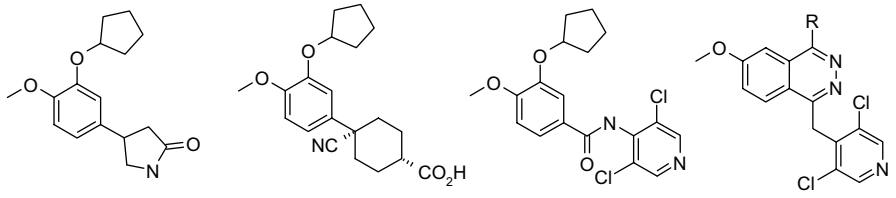

Rolipram Ariflo Piclamilast Phthalzine based inhibitors

Keywords: PDE IV inhibitors; Conformational analysis; NMR; Molecular dynamics.
* Corresponding author at present address: Chemistry Department, Inpharzam Ricerche SA, Via ai Söi, CH-6807 Taverne, Switzerland. Tel.: +41 91 935 45 18; fax: +41 91 935 45 12; e-mail: thomas.haack@zambongroup.com

0968-0896/$ - see front matter
doi:10.1016/j.bmc.2005.04.057

other inflammatory diseases.[2] Many inhibitors have been reported that are under clinical investigation.[3] The archetypal PDE IV inhibitor Rolipram was followed by several other compounds, most notably Ariflo and Piclamilast, replacing the pyrrolidinone of Rolipram with another functionality such as the dichloropyridine unit. However, the clinical utility of the pioneer compounds has been limited by side effects such as nausea, emesis and increased gastric acid secretion.[3]

We showed recently that the use of the phthalazine nucleus as a conformationally constrained analogue of Piclamilast was compatible with inhibitory potency.[4–6] This finding confirms our hypothesis that the carbonyl function of Rolipram and Piclamilast could be replaced by a π-bond of an aromatic ring and that a planar dihedral angle between the phenyl ring and the linker region of Rolipram-like analogues is allowed.[4] Nevertheless, these phthalazine derivatives showed a decreased potency compared to open amide, probably due to unfavourable interaction between the cyclopentyloxy and the *peri*-hydrogen in position 4 of the phthalazine nucleus (**1**).

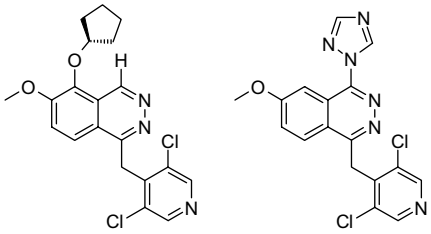

1 **2**

Subsequently, we were able to show that the catechol substitution pattern of Rolipram was not necessary for PDE IV potency if the cyclopentyloxy group is replaced by an appropriate group positioned at the heteroaromatic ring.[6] This finding finally leads to the observation that several heterocycles as cyclopentyloxy surrogates at position 4 of the phthalazine moiety are allowed. Most notably, derivative **2** with a triazole heterocycle was devoid of the common emetic side effect normally observed for the catechol rolipram-like compound class while maintaining good potency (241 nM) and an acceptable pharmacokinetic and safety profile.

In general, potential PDE IV inhibitors based on the phthalazine ring as scaffold showed activities from the low nanomolar to micromolar range.[4–6] The rationalisation of the structure–activity relationship of this class of compounds seemed rather difficult since polar substituents such as tertiary amines apolar groups such as phenyl residues showed comparable activity.[5] Very recently a comprehensive effort has been made to establish a three-dimensional quantitative structure–activity relationship of the homogeneous class of the phthalazine PDE IV inhibitors using the Comparative Molecular Field Analysis (CoMFA) method.[7] This method provides a correlation between both the electrostatic and steric field variations of the investigated molecules and their biological activity, allowing in principle the design of new and more potent compounds.

In the present contribution we report the results of a detailed conformational analysis of the phthalazine derivatives **2** to **5** representative of this class of novel PDE IV inhibitors. Compounds **2**, **3** and **5**, already disclosed in a prior publication,[5] show the identical 3′,5′-dichloro-4′-methylenepyridine substituent in position 1 of the phthalazine ring, while they differ for the five-membered ring heterocyclic substituents in position 4. The three compounds are characterised by very different biological activity in vitro with IC_{50} values ranging from 241 nM for **2** to 14 nM for **3** and to 17% at 10^{-7} M for **5**. Compounds **2** and **3** were also included in the data base of the above mentioned CoMFA analysis[7] and their markedly different activities were explained in terms of electrostatic field variations. In fact the model shows that the occurrence of electronegative atoms in the internal positions 1″, 2″ or 5″ of the pentacyclic ring induces an activity enhancement of the molecule, while the inhibitory potency decreases when the electronegative atoms are located in the external positions 3″ and (or) 4″. In this work we use a combination of computational methods and NMR experiments to describe in detail the conformational behaviour of the selected molecules with the aim of determining the preferential position or motion of the electronegative atoms of the five-membered ring and eventually their correlation with the biological activity. For compound **2**, a complete single crystal structure was also obtained, thus providing a relation between its conformational properties in the solid state and in solution. In addition, a newly synthesised compound **4** bearing a monochloro-substituted methylenepyridine ring at carbon C-1 of phthalazine has also been examined. This compound shows a much lower PDE IV inhibition potency than the corresponding dichloroderivative **3** (IC_{50} of ca. 600 and 14 nM, respectively) and thus it may be worth investigating whether the structural variation is also accompanied by significant differences in the conformational behaviour.

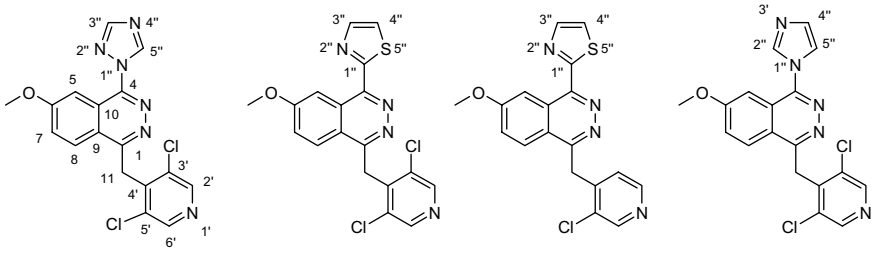

2 **3** **4** **5**

2. Results and discussion

2.1. Chemistry

The syntheses of compounds **2**, **3** and **5** bearing the dichloropyridine unit have been reported recently[5] but not of the monochloro compound **4**, presented as a substance without a synthetic scheme during the European chemistry symposium 2002.[8] Briefly, furanonecarboxylic acid **6** was prepared in two steps and in high yield from commercially available *m*-anisic acid by using an old procedure.[9] The key intermediates, the methylene furanones **8**, were obtained in high yields by acetic anhydride-induced condensation of **6** with pyridine aldehydes **7a** and **7b**,[10] as outlined in Scheme 1. The thiazole heterocycle of derivatives **3** and **4** was introduced prior to phthalazine formation under strong base conditions forming hemiketals **9**. Compound **9a** was yielded as a (7:2) mixture of *E*/*Z* diastereoisomers, whereas **9b** was pure *E*. The final phthalazines **3** and **4** were obtained after hydrazine cyclisation under acid catalysis. Crystallisation from an ethanol/DMF mixture yielded **4** as a light yellow solid, whereas **3** was a white solid.

Otherwise, imidazole or triazole heterocycles of derivatives **2** and **5**, respectively, were introduced after phthalazine formation, as outlined in Scheme 2. Briefly, key intermediate **8b** was cyclised by acid-catalysed hydrazinolysis (**10**) and chlorinated by $POCl_3$ to yield the corresponding chloro derivative **11**, which subsequently was treated with the preformed heterocycle anion to yield the final products **2** and **5**.

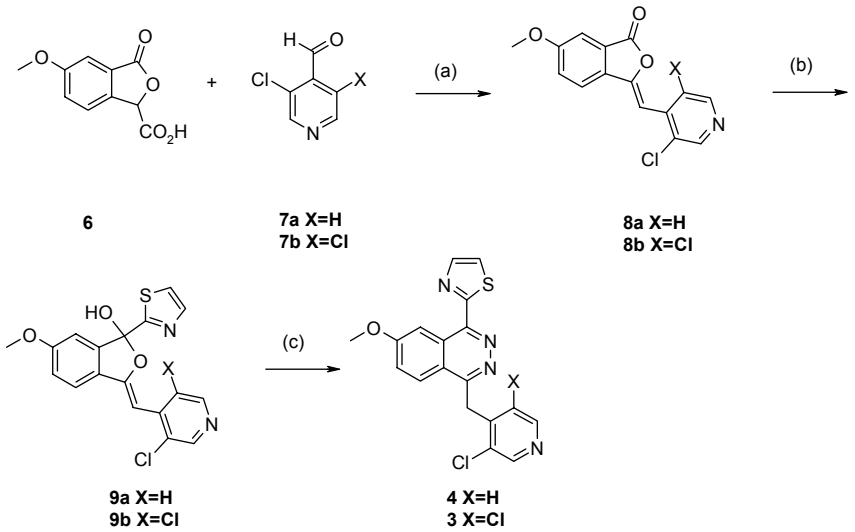

Scheme 1. Synthesis of thiazole compounds **3** and **4**. Reagents and conditions: (a) acetic anhydride, toluene, reflux, 10 h, (70% X=H, 99% X=Cl); (b) 2-bromothiazole, LDA, −78 °C, 2 h, −65 °C, 27% (X=H), 38% (X=Cl); (c) hydrazine hydrate, MeOH, AcOH, reflux, 6 h, 70% (X=H), 60% (X=Cl).

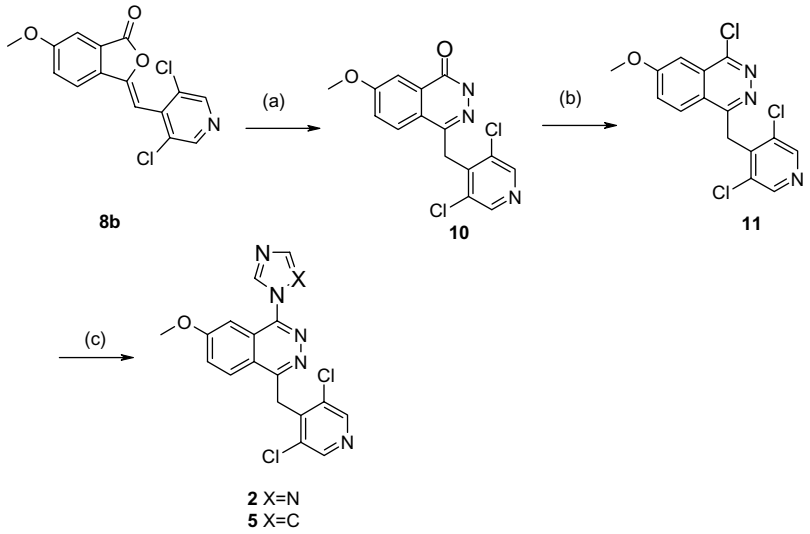

Scheme 2. Synthesis of triazole compound **2** and imidazole-containing compound **5**. Reagents and conditions: (a) hydrazine hydrate, MeOH, AcOH, reflux, 2 h, 99%; (b) $POCl_3$, reflux, 4 h, 94%; (c) imidazole or triazole, NaH, DMF, 100 °C, 20 h, 53% **2**, 50% **5**.

2.2. NMR and simulation methods

2.2.1. Conformational behaviour of the chloropyridine unit. The phthalazine derivatives **2**–**5** here examined display only two regions of potential flexibility: that of the chlorosubstituted pyridine residue (rotation about C_1/C_{11} and $C_{11}/C_{4'}$ bonds) and that of the five-membered ring (rotation about the bond C_4/pentacycle).

The X-ray study performed on **2** (Fig. 1) showed that the dichloropyridine unit is orthogonal to the plane of the phthalazine ring ($\Psi = 93.4°$) and oriented towards the external nitrogen atom N_2. The dihedral angle Φ is close to 180°, so that the four atoms are nearly planar and the methylene hydrogens H_{11} point towards the benzenic proton H_8 with distances H_{11}/H_8 of 2.34 and 2.48 Å.

In solution the conformational preference of the dichloropyridine residue may be investigated by determining the interproton distances H_8–H_{11} from NOE measurements. The two methylene protons H_{11a} and H_{11b} are magnetically equivalent and give rise to a singlet in the spectrum, thus only the mean distance H_8–H_{11} can be determined. Such distance is very different from the arithmetic mean since physically the averaging process occurs over the inverse sixth power of the internuclear distances.[11] Therefore, the experimental result provides

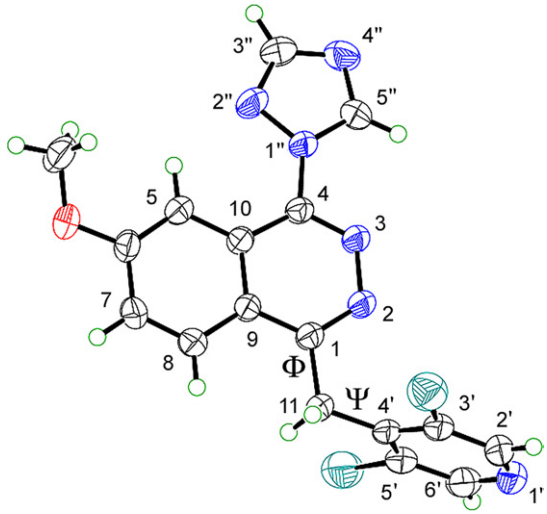

Figure 1. ORTEP drawing of the X-ray structure of **2**. Φ and Ψ are the dihedral angles defined by C_9–C_1–C_{11}–$C_{4'}$ and by C_1–C_{11}–$C_{4'}$–$C_{5'}$, respectively.

Table 1. Mean values of the apparent distance H_8–H_{11} determined from NOE data[a]

Sample	$r_{8,11}$ (Å) ($CDCl_3$)	$r_{8,11}$ (Å) (DMSO)
2	2.46	2.40
3	2.50	2.40
4	2.45	—[b]
5	2.48	2.42

[a] Mean of three measurements; estimated precision ±0.1 Å.
[b] Not measured due to the low solubility of **4** in DMSO.

Table 2. Dihedral angles[a]

Dihedral angle	**2**	**3**	**4**	**5**
Φ	60.9°	61.2°	−66.2°	−61.0°
Ψ	125.7°	−125.3°	129.6°	125.6°
Π	86.6°	−16.3°	16.8°	−113.5°

[a] $\Phi = C_9$–C_1–C_{11}–$C_{4'}$; $\Psi = C_1$–C_{11}–$C_{4'}$–$C_{5'}$; $\Pi = C_{10}$–C_4–$X_{1''}$–$X_{2''}$ Φ, Ψ and Π at the absolute energy minimum obtained through the MD simulations of compounds **2**–**5** performed in vacuo.

an apparent distance, which mainly reflects the distance between H_8 and the nearest H_{11} hydrogen. The data obtained in $CDCl_3$ and DMSO solutions are collected in Table 1. Within the experimental errors (estimated precision ±0.1 Å) the H_8–H_{11} apparent distance is ca. 2.47 Å in chloroform and ca. 2.40 Å in DMSO (values averaged over the four compounds). This result indicates that the conformation of the substituent at the phthalazine carbon C_1 is the same for compounds **2**–**5**, including compound **4** also which bears only one chlorine substituent on the pyridine ring. The apparent distance H_8–H_{11} determined in the solution is similar to that measured in the solid state for **2** (mean value 2.41 Å) suggesting that the pyridine ring points towards the external part of the phthalazine nucleus in both cases. On the other hand, the angle Φ, which is close to 180° for **2** in the solid state with the atoms N_2 and $C_{4'}$ practically eclipsed, is reasonably expected to have values of ca. ±120° in solution to release the steric hindrance.

However, the molecular dynamics simulations suggest a more complicated situation. The Φ and Ψ torsion angles for the conformations with the global energy minimum in vacuo are mentioned in Table 2. In the dielectric medium, the values of Φ and Ψ are equal to those shown in the table to within ± 0.5°, while in water they differ by up to 4°, indicating very little solvent effects. The Φ values are very close to 60°, while those of Ψ occur at about 120°. As a result, the dichloropyridine ring is approximately orthogonal to the phthalazine plane, but oriented towards the internal part of the phthalazine nucleus, unlike what is suggested above. Correspondingly, the distances H_8–H_{11} are about 2.4–2.5 and 3.8 Å for all compounds. If the molecules existed in this fixed conformation, the average distance probed by the NOE measurements should be 2.72 Å, using the expression[11] $r^{-6}_{H_8-H_{11}} = (r^{-6}_{H_8-H_{11a}} + r^{-6}_{H_8-H_{11b}})/2$, a value substantially different from the experimental one. However, the energy difference between the internal and the external arrangement of the pyridine ring (the global and a local energy minimum, respectively) amounts to about 1.5 kcal/mol. Moreover, the energy barrier separating these minima is about 2.7 kcal/mol only, so that they are both visited relatively often at room temperature. Interestingly, the PDF $g_{H_8-H_{11}}(r)$, reported in Figure 2 for compound **2** as a typical case, shows that during the MD simulations the most probable hydrogen separations are about 2.4–2.5 and 3.8 Å. However, the broader distribution for the closer hydrogens (filled symbols) should be noted, since it indicates that this distance can be even smaller than 2 Å, thanks to thermal fluctuations. Therefore, we calculated the weighted average

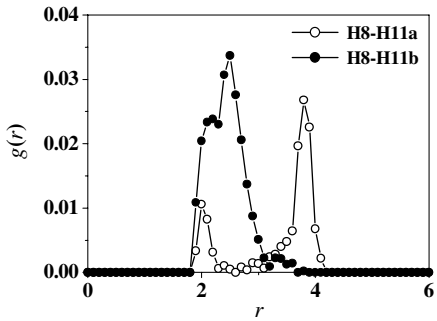

Figure 2. The pair distribution function (PDF) for the distances r (in Å) between hydrogen H_8 and the methylene hydrogens H_{11a} and H_{11b} for compound **2**.

value $\bar{r}_{H_8-H_{11}}$ as above using the averages $\bar{r}_{H_8-H_{11a}}$ and $\bar{r}_{H_8-H_{11b}}$ obtained from the appropriate volume integrals involving the separate PDFs. The resulting value is 2.57 Å for compound **2**, being marginally larger for other compounds. Such values, although still larger than the experimental ones, are now closer to the distances determined in chloroform.

In conclusion, the MD simulations show for all compounds that in the most stable conformation the pyridine ring is oriented towards the internal part of the phthalazine nucleus, but indicate at the same time that frequent transitions occur towards the external conformation. The NOE data are roughly in agreement with the MD calculations, suggesting however that the latter conformation is more populated than predicted by the simulations. It is worth noting that compounds **3** and **4**, which only differ for the number of chlorine atoms on the pyridine ring, show a strictly similar conformational behaviour. Thus, the markedly different activity between these two PDE IV inhibitors (IC_{50} of 14 and ca. 600 nM, respectively) depends exclusively on the different substitution pattern of the pyridine ring. This is an interesting finding, making plausible a possible interaction between one of the two chlorine atoms with the zinc metal ion found in the active site of PDEIV. Thus, the role of disubstitution could be viewed as enhancement of the local chlorine concentration.

2.2.2. Conformational properties of the five-membered rings. The five-membered ring attached to carbon C_4 of phthalazine has a single conformational degree of freedom, the rotation around the bond connecting C_4 to the pentacycle. Such rotation moves about in the space the electronegative heteroatoms of the ring, thus strongly influencing the distribution of the electrostatic fields in this part of the molecule. The conformational preferences of the pentacycle are dictated by the energy maxima corresponding to the coplanarity with the phthalazine ring due to steric interactions with '*ipso*' proton H_5 and to the orthogonality of the rings due to the loss of π conjugation. The steady state NOE enhancements between the phthalazine hydrogen H_5 and the protons located on the pentacycle have been measured to gain information on the preferential orientation of the ring with respect to the phthalazine plane.

Table 3. Steady state NOE enhancements measured on the five-membered ring hydrogens by irradiation of H_5 of phthalazine ring

Sample	H-2″ (%)	H-3″ (%)	H-4″ (%)	H-5″ (%)
2		1.2[a]		1.5[a]
		2.3[b]		2.6[b]
		1.2[c]		1.5[c]
3		1.5[a]		ND[a]
		2.0[b]		ND[b]
4		1.4[a]		ND[a]
5	5.9[d]		ND[d]	7.2[d]

[a] $CDCl_3$.
[b] DMSO-d_6.
[c] CD_3OD.
[d] C_6D_6/CD_3OD 1:1.

The experimental data are collected in Table 3 as percent enhancements of the signals.

The X-ray analysis of **2** shows that in the solid state the triazole ring is almost coplanar with the nitrogen atom $N_{2''}$ oriented towards the proton H_5 of the phthalazine nucleus (dihedral angle $\Pi = C_{10}–C_4–N_{1''}–N_{2''}$ of −1.2° and distance $H_5/N_{2''}$ of 2.24 Å) (Fig. 1). In solution such conformation no longer exists. In fact both $H_{3''}$ and $H_{5''}$ protons of the pentacycle display weak NOEs with enhancements in the range 1.2–2.6% upon irradiation of H_5 (Table 3). The experiment was carried out in different solvents to test whether significant variations occur depending on the dielectric constant of the medium. For each solvent, $H_{3''}$ and $H_{5''}$ display similar enhancements suggesting that the triazole ring in solution is strongly rotated with respect to the phthalazine plane. Therefore, the distance $H_5–H_{5''}$ decreases while the distance $H_5–H_{5''}$ decreases while the distance $H_5–H_{3''}$ increases compared to those in the coplanar conformation, so that a NOE is observed on both nuclei. The MD calculations confirm the qualitative conclusions inferred from NOE data in all the simulation environments. The PDF is the best way to represent the distribution of the internuclear distances. These functions calculated for the distances $H_5–H_{3''}$ and $H_5–H_{5''}$ of **2** are reported in Figure 3a for the simulations in vacuo. The distribution of distance $H_5–H_{5''}$ is rather broad with a maximum probability at about 3.2 Å, while the distribution of distance $H_5–H_{3''}$ is somewhat sharper with a maximum probability centred around 4.5 Å. The Π dihedral angle for the global minimum energy conformation of **2** (see Table 3) indicates that the pentacycle is orthogonal to the phthalazine plane, independent of the simulation environment.

Compounds **3** and **4** have the identical 1,3-thiazole substituent at carbon C_4 and show very similar NOE enhancements. By irradiation of H_5 only the hydrogen $H_{3''}$ is affected, while $H_{4''}$ does not show any effect indicating that in this case the five-membered ring in solution adopts a conformation with the nitrogen atom strongly oriented towards the inner part of the phthalazine moiety. The PDF functions calculated for the distances $H_5–H_{3''}$ and $H_5–H_{4''}$ (Fig. 3b) show sharp peaks with maximum probability at 4.1 Å for $H_5–H_{3''}$ and 5.7 Å for $H_5–H_{4''}$. The Π dihedral angle for conformation of **3** and **4** with the global minimum energy in vacuo

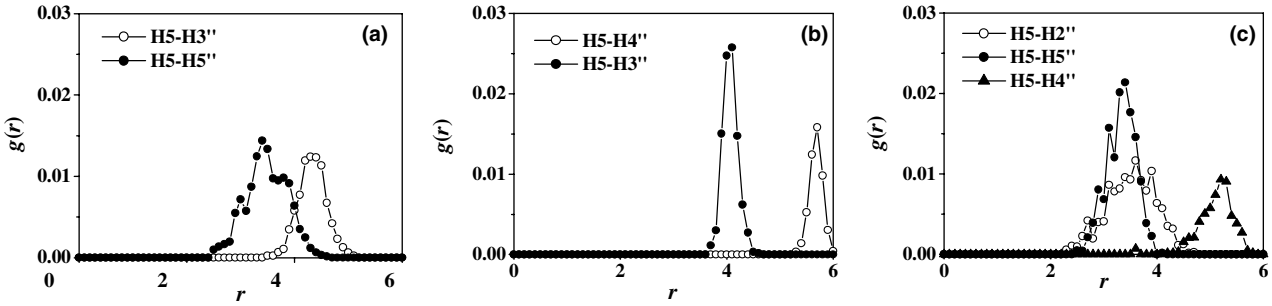

Figure 3. The pair distribution functions for the distances r (in Å) between proton H_5 and the hydrogens located on the pentacyclic ring for compounds **2** (a), **3** (b) and **5** (c). The plot for compound **4** is not shown for brevity being the same as for compound **3**.

is about 16–17°, indicating that in this case the pentacycle and phthalazine ring are not too far from coplanarity. In this case, polar effects and/or hydrogen bonds with water lead to somewhat larger effects on Π with a difference between the various simulation media being anyway comprised within ±10°.

In compound **5**, the 1,3-diazole ring is the substituent at carbon C_4 of the phthalazine nucleus. The irradiation of H_5 produces strong enhancements on protons $H_{2''}$ and $H_{5''}$ (5.9% and 7.2%, respectively), without any effect on $H_{4''}$. In this case, we can reasonably expect that the diazole ring makes large-amplitude oscillations about the C_4–$N_{1''}$ bond, which in turn brings both hydrogens near H_5. In fact, the PDF functions show the occurrence of two broad distance distributions with maximum probability around 3.5 Å (Fig. 3c), whereas $H_{4''}$ is much further away at about 5 Å. For this molecule, the preferred conformation shows in vacuo a Π value of −114°, and in water of −104°, much closer to orthogonality than in compounds **3** and **4**.

3. Conclusion

In conclusion, the combined information from the NOE data of the protons located on the five-membered rings and the MD calculations indicates that the thiazole substituent has a well defined conformation, as indicated also by the sharp peaks of the PDF's of Figure 3b. In these compounds, the thiazole ring is almost coplanar with the phthalazine nucleus, with the nitrogen atom located near H_5. Moreover, in vacuo the rotated conformation bringing the S atom close to H_5 represents a local energy minimum for $\Pi = \pm 155°$, which is less stable than the global one by 4.5 kcal/mol and is separated by an energy barrier larger than 11 kcal/mol; thus it is unlikely to be of any significance. On the other hand, both the diazole and triazole rings exist in a broad distribution of conformational states with large distribution of the dihedral angles, and correspondingly with broad PDF's of Figure 3a and c.

As outlined above, compounds **2**, **3** and **5**, which differ in the structure of the pentacyclic substituent at carbon C_4 of the phthalazine nucleus, are characterised by markedly different activities as PDE IV inhibitors. Such differences have been explained by Chakraborthi et al. using CoMFA[7] in terms of the position of the electronegative nitrogen atoms in the five-membered ring: these atoms produce an increase of the biological activity when located in the internal positions while in the external positions they induce a decrease of the activity. In the present study it appears that the active and nonactive molecules differ strongly also in the conformational behaviour of the pentacyclic ring. In the most active compound **3**, the thiazole ring has a well-defined conformation with the nitrogen atom oriented towards the benzene moiety and a modest deviation from strict coplanarity with the phthalazine moiety. On the contrary, the diazole and triazole rings of the less active molecules **2** and **5** show a much greater rotational freedom with strong deviations from coplanarity with the phthalazine nucleus, becoming almost orthogonal. Thus, we suggest that some coplanarity of heterocycles at position 4 of the phthalazine moiety is important for PDE IV activity.

4. Experimental

4.1. General methods

NMR spectra were run on Bruker ARX 400 or Bruker Avance 500 spectrometers. Chemical shifts are in δ from internal TMS (tetramethylsilane).

4.2. NMR

The distance ratio $r(H_8, H_{11})/r(H_7, H_8)$ of compounds **2**–**5** was determined from the phase-sensitive NOESY spectra. For each solution the proton relaxation times T_1 were measured to choose the appropriate mixing and pulse repetition times. The T_1 values range from 0.7 to 1.0 s of the CH_2–11 hydrogens to 5–9 s of the most isolated nuclei of the pyridine and five-membered rings. Thus the NOESY spectra were obtained using a quite short mixing time of 0.2–0.3 s due to the short CH_2–11 T_1 and a relaxation delay of 10–15 s dictated by the rather long T_1 of H-7 (2.0–3.4 s). In these conditions the cross peak intensities a_{ij} are proportional to the cross relaxation rates σ_{ij}, which in turn are related to the internuclear distances r_{ij} by the equation:[11]

$$\sigma_{ij} = (\hbar^2\gamma^4/2r_{ij}^6)\tau_c$$

where γ is the proton magnetogyric ratio and τ_c the correlation time of the internuclear vector H_i–H_j. With the

assumption that the correlation time τ_c is equal for all molecular internuclear vectors the distance ratios can be obtained directly from the ratio of the cross-peak intensities:[11]

$$r_{ij}/r_{ki} = (a_{ki}/a_{ij})^{1/6}$$

This equation, provided r_{ki} is known, allows one to obtain the unknown distance r_{ij}. The distance $r(H_8, H_{11})$ estimated with this method is an apparent distance due to the magnetic equivalence of the methylene protons and mainly reflects the distance between H_8 and the nearest H_{11} hydrogen. For all compounds **2**–**5** the H_7–H_8 distance of 2.41 Å as determined by the modelling calculations was chosen as the reference distance.

The steady state NOE difference experiments were carried out by acquiring both on- and off-resonance spectra using a 75 dB attenuation of the decoupling power. This experiment was employed to investigate the spatial disposition of the five-membered rings with respect to the phthalazine moiety. As the T_1 values of the hydrogens on five-membered rings are rather long (5–9 s), an irradiation time of 30–40 s was used to reach with certainty the steady state and detect also very small NOE enhancements.

The NMR spectra of compounds **2**–**5** were obtained in $CDCl_3$ and DMSO-d_6 solutions.

Compound **2**: ^{1}H NMR ($CDCl_3$): δ 8.49 (1H, d, J = 2.6 Hz, H_5), 7.68 (1H, dd, J = 2.6 and 9.2 Hz, H_7), 8.23 (1H, d, J = 9.2 Hz, H_8), 4.96 (2H, s, H_{11}), 4.04 (3H, s, OCH_3), 8.55 (2H, s, $H_{2',6'}$), 8.27 (1H, s, $H_{3''}$), 9.23 (1H, s, $H_{5''}$); ^{1}H NMR (DMSO-d_6): δ 7.96 (1H, d, J = 2.6 Hz, H_5), 7.87 (1H, dd, J = 2.6 and 9.2 Hz, H_7), 8.63 (1H, d, J = 9.2 Hz, H_8), 5.07 (2H, s, H_{11}), 3.97 (3H, s, OCH_3), 8.69 (2H, s, $H_{2',6'}$), 8.49 (1H, s, $H_{3''}$), 9.38 (1H, s, $H_{5''}$); ^{13}C NMR (DMSO-d_6): δ 156.8 (C_1), 149.4 (C_4), 104.7 (C_5), 163.4 (C_6), 126.0 (C_7), 127.8 (C_8), 123.3 and 123.2 (C_9, C_{10}), 34.4 (C_{11}), 56.9 (OCH_3), 147.9 ($C_{2',6'}$), 133.8 ($C_{3',5'}$), 143.9 ($C_{4'}$), 146.3 ($C_{3''}$), 154.1 ($C_{5''}$).

Compound **3**: ^{1}H NMR ($CDCl_3$): δ 9.36 (1H, d, J = 2.6 Hz, H_5), 7.61 (1H, dd, J = 2.6 and 9.2 Hz, H_7), 8.18 (1H, d, J = 9.2 Hz, H_8), 4.95 (2H, s, H_{11}), 4.08 (3H, s, OCH_3), 8.53 (2H, s, $H_{2',6'}$), 8.06 (1H, d, J = 3.3 Hz, $H_{3''}$), 7.50 (1H, d, J = 3.3 Hz, $H_{4''}$); ^{1}H NMR (DMSO-d_6): δ 9.22 (1H, d, J = 2.4 Hz, H_5), 7.82 (1H, dd, J = 2.4 and 9.2 Hz, H_7), 8.56 (1H, d, J = 9.2 Hz, H_8), 5.04 (2H, s, H_{11}), 4.05 (3H, s, OCH_3), 8.67 (2H, s, $H_{2',6'}$), 8.19 (1H, d, J = 3.3 Hz, $H_{3''}$), 7.96 (1H, d, J = 3.3 Hz, $H_{4''}$); ^{13}C NMR ($CDCl_3$): δ 155.3 (C_1), 150.2 (C_4), 106.8 (C_5), 163.8 (C_6), 125.7 (C_7), 125.6 (C_8), 126.9 and 122.3 (C_9, C_{10}), 34.7 (C_{11}), 56.7 (OCH_3), 148.1 ($C_{2',6'}$), 134.4 ($C_{3',5'}$), 143.6 ($C_{4'}$), 144.7 ($C_{3''}$), 122.9 ($C_{4''}$).

Compound **4**: ^{1}H NMR ($CDCl_3$): δ 9.33 (1H, d, J = 2.6 Hz, H_5), 7.50 (1H, dd, J = 2.6 and 9.2 Hz, H_7), 7.94 (1H, d, J = 9.2 Hz, H_8), 4.81 (2H, s, H_{11}), 4.06 (3H, s, OCH_3), 8.31 (1H, d, J = 4.9 Hz, $H_{2'}$), 7.07 (1H, d, J = 4.9 Hz, $H_{3'}$), 8.62 (1H, s, $H_{6'}$), 8.09 (1H, d, J = 3.3 Hz, $H_{3''}$), 7.54 (1H, d, J = 3.3 Hz, $H_{4''}$); ^{1}H NMR (DMSO-d_6): δ 9.19 (1H, d, J = 2.6 Hz, H_5), 7.73 (1H, dd, J = 2.6 and 9.2 Hz, H_7), 8.33 (1H, d, J = 9.2 Hz, H_8), 4.87 (2H, s, H_{11}), 4.01 (3H, s, OCH_3), 8.44 (1H, d, J = 4.7 Hz, $H_{2'}$), 7.32 (1H, d, J = 4.7 Hz, $H_{3'}$), 8.65 (1H, s, $H_{6'}$), 8.20 (1H, d, J = 3.2 Hz, $H_{3''}$), 7.99 (1H, d, J = 3.2 Hz, $H_{4''}$); ^{13}C NMR ($CDCl_3$): δ 156.6 (C_1), 149.9 (C_4), 106.2 (C_5), 163.4 (C_6), 125.2 (C_7), 126.6 (C_8), 126.6 and 121.9 (C_9, C_{10}), 36.7 (C_{11}), 56.7 (OCH_3), 149.7 ($C_{6'}$), 145.0 and 131.9 ($C_{4'}$, $C_{5'}$), 148.1 ($C_{2'}$), 125.4 ($C_{3'}$), 144.2 ($C_{3''}$), 122.5 ($C_{4''}$).

Compound **5**: ^{1}H NMR ($CDCl_3$): δ 7.32 (1H, d, J = 2.6 Hz, H_5), 7.67 (1H, dd, J = 2.6 and 9.2 Hz, H_7), 8.23 (1H, d, J = 9.2 Hz, H_8), 4.95 (2H, s, H_{11}), 3.96 (3H, s, OCH_3), 8.55 (2H, s, $H_{2',6'}$), 8.05 (1H, s, $H_{2''}$), 7.27 (1H, d, J = 1.6 Hz, $H_{4''}$), 7.49 (1H, d, J = 1.6 Hz, $H_{5''}$); ^{1}H NMR (DMSO-d_6): δ 7.26 (1H, d, J = 2.6 Hz, H_5), 7.85 (1H, dd, J = 2.6 and 9.1 Hz, H_7), 8.62 (1H, d, J = 9.1 Hz, H_8), 5.04 (2H, s, H_{11}), 3.97 (3H, s, OCH_3), 8.69 (2H, s, $H_{2',6'}$), 8.32 (1H, s, $H_{2''}$), 7.25 (1H, d, J = 1.4 Hz, $H_{4''}$), 7.88 (1H, d, J = 1.4 Hz, $H_{5''}$); ^{13}C NMR (C_6D_6/CD_3OD 1:1): δ 156.2 (C_1), 150.3 (C_4), 102.9 (C_5), 164.2 (C_6), 126.1 (C_7), 127.1 (C_8), 126.1 and 123.5 (C_9, C_{10}), 34.4 (C_{11}), 56.0 (OCH_3), 147.8 ($C_{2',6'}$), 134.5 ($C_{3',5'}$), 143.9 ($C_{4'}$), 138.3 ($C_{2''}$), 130.0 ($C_{4''}$), 120.9 ($C_{5''}$).

4.3. Computer simulations

All simulations were performed with InsightII/Discover,[12] using the consistent valence force field CVFF[13] with a Morse potential for the bonded atoms. The initial geometries, generated through the available library fragments, were fully minimised up to an energy gradient lower than 10^{-3} kcal mol^{-1} Å^{-1}. The molecular dynamics simulations at 300 K were performed (i) in vacuo, (ii) into an effective dielectric medium mimicking water using a distance-dependent dielectric constant and (iii) in the explicit presence of the solvent, using a large number of water molecules at a density of 1 g cm^{-3} with periodic boundary conditions. The temperature was controlled through the Berendsen thermostat, and the dynamical equations were integrated through the Verlet algorithm with a timestep of 1 fs. After an initial equilibration of 30 ps, the data collection was carried out for 500 ps, and a large number of instantaneous structures was optimised in search of the global energy minima. These geometries were subjected to a systematic dihedral search, first by changing the dihedral angles defined by atoms C_9–C_1–C_{11}–$C_{4'}$ and C_1–C_{11}–$C_{4'}$–$C_{5'}$ (Φ and Ψ, respectively), for a total of 1369 conformations, and then by changing the Π dihedral angle around the bond connecting the five-membered ring to the phthalazine nucleus defined by atoms $X_{2''}$–$X_{1''}$–C_4–C_{10} (X = N or C; see Scheme 1), for a total of 73 conformations. The geometries sampled in the MD runs were analysed through the pair distribution function $g_{ij}(r)$ (or PDF for short). This function gives the probability density of finding atoms j at a distance comprised between r and $r + dr$ from atoms i, and is defined as $g_{ij}(r) = d\langle N_{ij}(r)\rangle/\rho_j \cdot dV(r)$. Here, $d\langle N_{ij}(r)\rangle$is the average number of times the j atoms are comprised in a spherical

shell of thickness dr and volume d$V(r)$ at a distance r from atoms i, and ρ_j is their bulk density. For molecules in vacuo or in a dielectric medium, ρ_j is set to 1. In the text, we mainly discuss the results obtained in vacuo, because they better approximate the solvents used in the NMR measurements, since both $CDCl_3$ and DMSO are weakly complexating solvents, and anyway cannot form hydrogen bonds, unlike water. Moreover, $CDCl_3$ has a very low dielectric constant ($\varepsilon = 4.8$), hence it is reasonably approximated by the simulations in vacuo, whereas DMSO has a larger value ($\varepsilon = 45$), though not as large as water. Therefore, use of the latter solvent in the simulations corresponds to a limiting case. Anyway, in all cases the overall conformational features were independent of the simulation medium, with only minor quantitative differences.

4.4. Synthesis

4.4.1. Material and methods. ^{1}H NMR spectra were recorded as $CDCl_3$ or DMSO-d_6 solutions on a Varian Gemini 200 MHz spectrometer. Chemical shifts are reported in parts per million (δ units) relative to $CHCl_3$ or DMSO as internal standards (in NMR descriptions; s = singlet, d = doublet, t = triplet, q = quartet, m = multiplet, and br = broad peak).

ESI mass spectra were recorded with a Finnigan Aqa mass spectrometer (electron spray, positive ionisation) connected to a Gilson HPLC.

Reactions were followed either by reverse phase HPLC/MS (Gilson Auto purifier, C18 column Zorbax SBC18 (3.5 μm, 2.1 × 50 mm, DAD detector) or thin-layer chromatography conducted on precoated silica gel 60F254 plates (Merck). Chromatography was performed on 100–200 mesh silica gel C-200 (Wako Pure Chemical) using the solvent systems (volume ratios) indicated below.

4.4.2. 3-Chloro-4-formyl-pyridine (7). 3-Chloropyridine (4 g, 35.22 mM) in THF (8 mL) was added to 2 M LDA (19.4 mL, 38.7 mM) in THF (50 mL) under Argon atmosphere at −65 °C and stirred for 30 min. Subsequently, ethylchloroformate (2.86 g, 38.7 mM) in THF (8 mL) was added and the resulting mixture stirred at −65 °C for 2 h. The reaction was stopped by quenching the solution with saturated NH_4Cl and THF at ambient mixture. Work-up of the solution was done by addition of water, extraction with EtOAc, washing with brine, drying (Na_2SO_4) and evaporation to dryness. The crude product was purified by chromatography on silica gel using petroleum ether/EtOAc (7/3) as eluant to provide the product (2 g, 40%) as a white solid. ESI$^+$ MS for C_6H_4ClNO calcd (141.56) 141, 141.9 (MH$^+$) found. ^{1}H NMR ($CDCl_3$): δ 10.50 (s, 1H), 8.78 (s, 1H), 8.67 (d, 1H, $J = 4.9$ Hz), 7.68 (d, 1H, $J = 4.9$ Hz).

4.4.3. 3-(3-Chloro-pyridin-4-ylmethylene)-6-methoxy-3*H*-isobenzofuran-1-one (8a). Acetic anhydride (1.05 mL) was added to a stirred mixture of **6** (700 mg, 3.36 mM) and **7a** (524 mg, 3.7 mM) in toluene (5 mL). The mixture was heated at reflux for 10 h, cooled down to room temperature and filtered to provide pure trans **8** (680 mg, 70%) as a white solid. ESI$^+$ MS for $C_{15}H_{10}ClNO_3$ calcd (287.70) 287, 288.0 (MH$^+$) found. ^{1}H NMR ($CDCl_3$): δ 8.58 (s, 1H), 8.47 (d, 1H, $J = 5.5$ Hz), 8.11 (d, 1H, $J = 5.5$ Hz), 7.74 (d, 1H, $J = 8.3$ Hz), 7.3 (d, 1H, $J = 8.3$ Hz), 6.61 (s, 1H), 3.90 (s, 3H).

4.4.4. 3-(3,5-Dichloro-pyridin-4-ylmethylene)-6-methoxy-3*H*-isobenzofuran-1-one (8b). Acetic anhydride (60 mL) was added to a stirred mixture of **6** (12.4 g, 60 mmol) and **7b** (10.8 g, 61 mmol) in toluene (150 mL). The mixture was heated at reflux for 0.5 h, cooled down to room temperature and evaporated. The residue was three times dissolved in 50 mL toluene and evaporated yielding trans **8** (19.2 g, quantitative) as a yellow solid pure enough to be used in the following steps. ESI$^+$ MS for $C_{15}H_9Cl_2NO_3$ calcd (322.15) 321, 322.0 (MH$^+$) found. ^{1}H NMR ($CDCl_3$): δ 8.60 and 8.50 (s, 2H), 7.77–6.20 (m, 4H), 3.90 (s, 3H).

4.4.5. 3-(3-Chloro-pyridin-4-ylmethylene)-6-methoxy-1-thiazol-2-yl-1,3-dihydro-isobenzofuran-1-ol (9a). *n*-BuLi (2.5 M in hexane, 2.64 mL,7.09 mmol) was added to 2-bromothiazole (1.06 g, 6.5 mmol) in Et_2O (30 mL) under argon atmosphere at −70 °C and stirred for 45 min. Subsequently, a solution of **8** (1.7 g, 5.91 mmol) in THF (70 mL) was added keeping the temperature at −65 °C. After 2 h the reaction was stopped by quenching with water and extracted with EtOAc. The organic phase was washed with water, dried (Na_2SO_4) and evaporated to dryness. The crude product was purified by chromatography on silica gel using petroleum ether/EtOAc (1/1) as eluant to provide **9a** (600 mg, 27%) as a yellow oil and as a mixture of 2:7 of *Z*:*E* isomers. ESI$^+$ MS for $C_{18}H_{13}ClN_2O_3S$ calcd (372.83) 372, 373.0 (MH$^+$) found. ^{1}H NMR ($CDCl_3$): δ *major product* (*E*): 8.32 (s, 1H), 8.20 (d, 1H, $J = 5.3$ Hz), 7.83 (d, 1H, $J = 8.3$Hz), 7.78 (d, 1H, $J = 3.4$ Hz), 7.40 (d, 1H, $J = 3.4$ Hz), 7.03 (m, 2H), 6.85 (d, 1H, $J = 2.26$ Hz), 5.15 (s, 1H), 3.84 (s, 3H); δ *minor product* (*Z*): 8.37 (s, 1H), 8.00 (d, 1H, $J = 5.3$ Hz), 7.80 (m, 2H), 7.45 (d, 1H, $J = 3.4$ Hz), 7.05 (m, 2H), 6.63 (d, 1H, $J = 2.26$ Hz), 5.00 (s, 1H), 3.84 (s, 3H).

4.4.6. 3-(3,5-Dichloro-pyridin-4-ylmethylene)-6-methoxy-1-thiazol-2-yl-1,3-dihydro-isobenzofuran-1-ol (9b). Same procedure as for **9a** except quantities: *n*-BuLi (2.5 M in hexane, 14.4 mL, 36 mmol), 2-bromothiazole (3 mL, 34.2 mmol) in Et_2O (17 mL) and the solution of **8** (10 g, 31 mmol) in THF (60 mL). The crude product was purified by chromatography on silica gel using petroleum ether/EtOAc (6/4) as eluant providing pure *E* **9b** (4.64 g, 38%) as a white solid. ESI$^+$ MS for $C_{18}H_{12}Cl_2N_2O_3S$ calcd (407.28) 406, 407.0 (MH$^+$) found. ^{1}H NMR ($CDCl_3$): δ 8.42 (s, 2H), 7.78 (d, 1H, $J = 5.3$ Hz), 7.88 (d, 1H, $J = 8.3$ Hz), 7.48 (d, 1H, $J = 3.4$ Hz), 7.10 (d, 1H, $J = 3.4$ Hz), 6.80 (d, 1H, $J = 4.9$ Hz), 5.38 (s, 1H), 3.84 (s, 3H).

4.4.7. 1-(3-Chloro-pyridin-4-ylmethyl)-6-methoxy-4-thiazol-2-yl-phthalazine (4). Hydrazine monohydrate was added to a stirred solution of **9a** (100 mg, 0.268 mmol) and acetic acid (0.077 mL, 1.34 mmol) in MeOH

(1 mL). The mixture was heated at reflux for 6 h, than cooled to room temperature, quenched with water and extracted with EtOAc. The organic phase was washed with water, dried (Na_2SO_4) and evaporated to dryness. The crude product was purified by silica chromatography using DCM/MeOH (98/2) as eluant providing **4** (70 mg, 70%) as light yellow solid. ESI^+ MS for $C_{18}H_{13}ClN_4OS$ calcd (368.85) 368, 369.0 (MH^+) found. ^1H NMR: see experimental part NMR.

4.4.8. 1-(3,5-Dichloro-pyridin-4-ylmethyl)-6-methoxy-4-thiazol-2-yl-phthalazine (3). Same procedure as **4** except quantities are hydrazine monohydrate (0.048 mL, 1 mmol) **9a** (125 mg, 0.302 mmol) and acetic acid (0.077 mL, 1.34 mmol) in MeOH (1.5 mL). The crude product was purified by silica chromatography using DCM/MeOH (98/2) as eluant providing **4** (72 mg, 60%) as a white solid. ESI^+ MS for $C_{18}H_{12}Cl_2N_4OS$ calcd (403.29) 402, 403.0 (MH^+) found. ^1H NMR: see experimental part NMR.

4.4.9. 1-(3,5-Dichloro-pyridin-4-ylmethyl)-7-methoxy-2*H*-phthalazin-1-one (10). Hydrazine monohydrate (18.4 mL, 0.378 mol) was added to a stirred suspension of **8b** (84.4 g, 0.126 mol) and acetic acid (15.4 mL) in MeOH (200 mL) under N_2 gas. The mixture was refluxed for 1 h, then left over night at rt and cooled over ice. The solid was filtered, washed with cold MeOH and dried in oven at 50 °C under vacuum yielding 33.3 g (80%) of pure **10**. ESI^+ MS for $C_{15}H_{11}Cl_2N_3O_2$ calcd (336.18) 335, 336.0 (MH^+) found. ^1H NMR ($CDCl_3$): δ: 12.34 (s, 1H), 8.64 (s, 2H), 8.19–7.54 (m, 3H), 4.58 (s, 2H), 3.95 (s, 3H).

4.4.10. 4-Chloro-1-(3,5-dichloro-pyridin-4-ylmethyl)-6-methoxy-phthalazine (11). Phosphorus oxychloride (22.2 mL, 0.230 mol) was added to a solution of **10** (10 g, 25.5 mmol) in acetonitrile (300 mL).The mixture was refluxed for 3 h, the solution concentrated, taken up in CH_2Cl_2 and extracted with Na_2CO_3 (pH 7–8). The organic phases were discoloured with charcoal, dried with Na_2SO_4 and concentrated to yield **11** in stoichiometric amounts. ESI^+ MS for $C_{15}H_{10}Cl_3N_3O$ calcd (354.63) 353, 354.0 (MH^+) found. ^1H NMR ($CDCl_3$): δ 8.50 (s, 2H), 8.13–7.54 (m, 3H), 4.88 (s, 2H), 4.04 (s, 3H).

4.4.11. 1-(3,5-Dichloro-pyridin-4-ylmethyl)-6-methoxy-4-(1,2,4)triazol-1-yl-phthalazine (2). NaH (0.084 g, 2.1 mmol, 60% in oil) was added to a solution of 1,2,4-triazole (0.19 g, 2.8 mmol) in dry DMF (10 mL) under N_2 and the mixture was heated to 40 °C for 1 h. The cooled solution was added to **11** (0.5 g, 1.4 mmol), heated overnight at 80 °C, poured into water (10 vol) and extracted three times with AcOEt. The organic phases were discoloured with charcoal, dried with Na_2SO_4 and evaporated to dryness. The crude material was purified by silica chromatography using AcOEt/PE (9/1) as eluant, and triturated in Et_2O, providing **4** (306 mg, 53%) as solid. ESI^+ MS for $C_{17}H_{12}C_{12}N_6O$ calcd (387.23) 386, 387.0 (MH^+) found. ^1H NMR: see experimental part NMR.

4.4.12. 1-(3,5-Dichloro-pyridin-4-ylmethyl)-6-methoxy-4-(1,4)imidazol-1-yl-phthalazine (5). Same procedure as **2** starting with NaH (0.120 g, 2.5 mmol, 60% in oil), 1,2,4-triazole (0.23 g, 3.4 mmol) in dry DMF (12 mL) and **11** (0.6 g, 1.7 mmol), which provide **5** (328 mg, 50%) as solid after chromatographic purification. ESI^+ MS for $C_{18}H_{13}Cl_2N_5O$ calcd (386.24) 385, 386.0 (MH^+) found. ^1H NMR: see experimental part NMR.

Acknowledgments

The authors thank Dr. Anthony Linden from the Institute of Organic Chemistry, University of Zürich, Switzerland for X-ray measurements and Mr. C. Riva for synthetic support. CCDC-258393 contains the supplementary crystallographic data for this paper. These data can be obtained free of charge via www.ccdc.cam.ac.uk/conts/retrieving.html (or from the Cambridge Crystallographic Data Centre, 12 Union Road, Cambridge CB2 1EZ, UK; fax: +44 1223 336033; e-mail: deposit@ccdc.cam.ac.uk).

References and notes

1. Torphy, T. *J. Am. J. Respir. Crit. Care Med.* **1998**, *157*, 351; Torphy, T. *J. Am. J. Respir. Crit. Care Med.* **1998**, *157*, 351.
2. Dyke, H. J.; Montana, J. G. *Expert Opin. Invest. Drugs* **1999**, *8*, 1301.
3. Norman, P. *Expert Opin. Ther. Pat.* **2002**, *12*, 93; Dyke, H. J.; Montana, J. G. *Expert. Opin. Invest. Drugs* **2002**, *11*, 1.
4. Napoletano, M.; Norcini, G.; Pellacini, F.; Marchini, F.; Ferlenga, P.; Pradella, L. *Bioorg. Med. Chem. Lett.* **2000**, *10*, 2235.
5. Napoletano, M.; Norcini, G.; Pellacini, F.; Marchini, F.; Morazzoni, G.; Ferlenga, P.; Pradella, L. *Bioorg. Med. Chem. Lett.* **2001**, *11*, 33.
6. Napoletano, M.; Norcini, G.; Pellacini, F.; Marchini, F.; Morazzoni, G.; Ferlenga, P.; Pradella, L. *Bioorg. Med. Chem. Lett.* **2002**, *12*, 5.
7. Chakraborthi, A. K.; Gopalakrishnan, B.; Sobhia, E. S.; Malde, A. *Bioorg. Med. Chem. Lett.* **2003**, *13*, 2473.
8. Moriggi, J.-D.; Macecchini, S.; Pippo, L.; Fattori, R.; Napoletano, M.; Fronza, G.; Raffaini, G.; Ganazzoli, F.; Haack, T. XVII European Medicinal Chemistry Symposium, 2002, poster number 243.
9. Chakhavarti, N. et al. *J. Chem. Soc.* **1929**, 196.
10. Bertini, V. et al. *Heterocycles* **1995**, *41*, 675.
11. *The Nuclear Overhauser Effect in Structural and Conformational Analysis*; Neuhaus, D., Williamson, M., Eds.; VCH: New York, 1989.
12. Accelrys Inc. InsightII 2000; Accelrys Inc.: San Diego, CA, 2000. See also the URL http://www.accelrys.com/.
13. Dauber-Osguthorpe, P.; Roberts, V. A.; Osguthorpe, D. J.; Wolff, J.; Genest, M.; Hagler, A. T. *Proteins: Struct., Funct., Genet.* **1988**, *4*, 31–47.